CAVITY PERTURBATION MEASUREMENT OF PLASMA DENSITY IN COMPLEX GEOMETRY RF DISCHARGES

by

R.M. Moroney, A.J. Lichtenberg, and M.A. Lieberman

Memorandum No. UCB/ERL M88/81

15 December 1988

CAVITY PERTURBATION MEASUREMENT OF PLASMA DENSITY IN COMPLEX GEOMETRY RF DISCHARGES

by

R.M. Moroney, A.J. Lichtenberg, and M.A. Lieberman

Memorandum No. UCB/ERL M88/81

15 December 1988

ELECTRONICS RESEARCH LABORATORY

College of Engineering
University of California, Berkeley
94720

CAVITY PERTURBATION MEASUREMENT OF PLASMA DENSITY IN COMPLEX GEOMETRY RF DISCHARGES

by

R.M. Moroney, A.J. Lichtenberg, and M.A. Lieberman

Memorandum No. UCB/ERL M88/81

15 December 1988

ELECTRONICS RESEARCH LABORATORY

College of Engineering
University of California, Berkeley
94720

Cavity perturbation measurement of plasma density in complex geometry rf discharges

R. M. Moroney, A. J. Lichtenberg, and M. A. Lieberman

Department of Electrical Engineering and Computer Science

and the Electronics Research Laboratory

University of California, Berkeley, California 94720

(Received

ABSTRACT

A non-invasive microwave diagnostic is used to determine the plasma density in a complex geometry rf discharge chamber. Experimentally determined relative spatial density and electric field profiles are used in Slater's perturbation equation to determine the peak and average density. Data have been obtained using several cavity modes and a wide range of pressures and powers. The measured peak densities are approximately a factor of two lower than those obtained from Langmuir probe measurements.

PACS number 52.70.Gw

I. INTRODUCTION

RF discharges have found many applications in materials processing, including sputtering, plasma etching and plasma enhanced chemical vapor deposition.[1] To understand and control the processes requires accurate measurement of important parameters such as electron density and temperature, ion velocity distribution, collisionality, etc. It is desirable to perform measurements with as little disturbance of the plasma as possible, i.e. not insert physical objects into the plasma. This is further required because processing plasmas are chemically active; thus such standard techniques as the use of Langmuir probes to measure the electron density are often difficult or inappropriate.

Alternative techniques for measuring plasma density, which are non-invasive, have employed microwave measurements.[2] Loss processes and the electron collision frequency have also been found by looking at the change in cavity Q of microwave resonances.[3,4] More recently, microwave techniques have been used to measure plasma lifetimes in reactive ion plasmas.[5,6] For irregularly shaped plasmas, the plasma density has been measured both by microwave cutoff[7] and cavity mode perturbation.[8] These mode perturbation measurements have generally been done on small volume plasmas compared to the resonant cavity volume.[2,3,8] Perturbation of simple cavity modes at low plasma density has also been used on large volume plasmas for determining the density.[5,9] Most cavity perturbation measurements have been used to measure densities with plasma frequency less than the probing microwave frequency. It has been shown, however, that if the skin depth of the plasma is larger than its characteristic length, then high density measurement is possible.[8] Theoretical work has been done investigating the range of validity of cavity perturbation density measurements.[10,11]

This paper presents cavity perturbation density measurements applied to a large volume,

low density plasma in a chamber with complex mode geometry. Experiments are performed in an rf excited argon plasma with pressures in the range 3–10 mT and powers in the range 1–100 W. Densities are found in the range 10^9 to 10^{10} cm^{-3}.

We use Slater's perturbation formula for the relative frequency shift,[12]

$$\frac{\Delta\omega}{\omega_0} = -\frac{1}{2}\frac{\int \mathbf{P}\cdot\mathbf{E}dV^*}{\int \epsilon_0|\mathbf{E}|^2 dV_0}, \tag{1}$$

where $\mathbf{E}$ is the unperturbed resonance electric field, $\mathbf{P}$ is the polarization, ω_0 is the unperturbed resonant frequency, the integral dV^* is over the plasma volume, and the integral dV_0 is over the total cavity volume. For an unmagnetized plasma in the frequency range where the plasma frequency $\omega_p << \omega_0$ and the collision frequency $\nu << \omega_0$, we can use (1) to relate the square of the average plasma frequency (proportional to the average electron density) to the relative shift in resonance frequency, $\Delta\omega/\omega_0$,[8]

$$\frac{\Delta\omega}{\omega_0} = \frac{1}{2\omega_0^2}\frac{\int \omega_p^2|\mathbf{E}|^2 dV^*}{\int |\mathbf{E}|^2 dV_0}. \tag{2}$$

In evaluating these integrals, most previous calculations have used cylindrical cavity modes such as the TM_{nm0} modes (for example, see[2,5,9]). In our discharge chamber, however, there are no pure cylindrical modes because of the complex geometry, shown in figure 1. We see that the electrode diameter is significantly smaller than the outer chamber diameter. Furthermore, the electrodes are positioned in a re-entrant geometry so that the concept of simple TE or TM cavity modes no longer applies. We have instead experimentally determined the electric field profiles of several modes. We have also measured the spatial density profile in order to evaluate the integral in the numerator of (2), although estimates of the profile would only slightly modify the results.

II . EXPERIMENTAL METHOD

Measurements are performed using an HP 8753A Network Analyzer and an HP 85044A Transmission/Reflection Test Set. These instruments are used to sweep an applied signal over a desired frequency range and measure the reflection and transmission coefficients from the plasma discharge chamber. The instruments greatly reduce the complexity of the experimental setup compared to, for example, Biondi and Brown.[2] The system is shown in figure 2. The excitation scheme consists of two small loops at the mid-plane of the chamber 180° apart along a diameter. Two glass inverted ports allow the loops to enter the chamber without being under vacuum. One of the loops introduces the applied signal, and the other receives the transmitted signal. Resonances are determined by peaks in the transmitted signal. The probing port positions at 45° and 90° from the loops are also shown.

Since we do not have simple TM_{nm0} modes in our discharge chamber, the electric field profiles of the modes are determined by measuring their frequency shifts versus the position of a small dielectric sphere. We use (1), evaluating the polarization $\mathbf{P}$ for a dielectric sphere of radius a and permitivity ϵ_1 immersed in a uniform electric field to obtain

$$\frac{\Delta\omega}{\omega_0} = -\frac{4\pi a^3 \epsilon_0 \frac{\epsilon_1-\epsilon_0}{\epsilon_1+2\epsilon_0} |\mathbf{E}(r_0,\phi_0,z_0)|^2}{2\epsilon_0 \int |\mathbf{E}|^2 dV_0}, \tag{3}$$

where (r_0, ϕ_0, z_0) is the location of the center of the sphere. Four different modes were used to measure densities, with resonant frequencies at 443 MHz, 506 MHz, 1.9 GHz and 2.6 GHz. We measure the radial variation of the electric field along diameters 45° and 90° from the loops, as shown by the dashed lines in figure 2. Because the spacing between the discharge plates is much smaller than the plate diameter and comparable to or smaller than a free space wavelength, we assume the electric field is uniform along z. For the higher frequency

resonances where lambda is on the order of the plate spacing (10 cm) this may not be a good assumption. The mode identification measurements are done at atmospheric pressure because of the support used to hold the dielectric sphere. The data for a particular mode are fitted to a simple functional form that is used when evaluating the integrals of equation (2). Since the perturbation equation is a variational formula, first order corrections in the electric field profile lead to only second order corrections in the frequency shift.

The spatial density variation of the plasma was determined from Langmuir probe measurements. The probe is moved in the r and z directions and the data normalized to the peak density. The normalized data are fit to a polynomial to obtain an expression for the density profile. In fact, the value of the average density is only weakly dependent on the polynomial form chosen, as will be shown in the data analysis. Thus the relative density measurements using Langmuir probes are not an essential part of the method.

Once the electric field and plasma density profile are known, the calculation of plasma density from the measured frequency shift is relatively straightforward. Langmuir probe measurements of the peak density were performed along with the microwave perturbation measurements for comparison.

III . RESULTS

Radial variations of the electric field were measured using a dielectric sphere (Silly Putty) 3 cm in diameter with $\epsilon_r \approx 5$ (this is approximate for unvulcanized rubber) on the end of a nylon rod. The ratio of chamber volume to sphere volume is estimated to be 500. The frequency shift of a mode is measured in the range $\Delta\omega/\omega_0 \approx 10^{-2}$–$10^{-3}$, and equation (3) leads to a value for $|\mathbf{E}|^2$. For the two high frequency resonances (1.9 GHz and 2.6 GHz), we have data along the 90° diameter shown in figures 3a and 3b, and assume that there is no variation with ϕ. For the two low frequency resonances (443 MHz and 506 MHz), we have $|\mathbf{E}|$ data along both the 45° and 90° diameters. As shown in figures 3c and 3d, the measurements give similar distributions with position, indicating that there is little or no variation in ϕ for either of these modes. Curve fits to these data are used to evaluate the integrals in (2).

Langmuir probe measurements of the density profile of discharges operating in the pressure range of 3–10 mT (about 1 Pa) and a power of 100 W have been made. The density profile versus z is plotted in figure 4, and versus r in figure 5. Polynomial fits are shown along with the data. In fitting the data, we assume that the density is equal to zero at the sheath edge, and that the r and z dependences are separable. The form of the density chosen to fit the data is

$$n = n_0\Big(1 - \big(\frac{z - Z_{max}}{Z_0}\big)^2\Big)\Big(1 - \big(\frac{r}{R_0}\big)^4\Big), \tag{4}$$

where the fitted constants for the data in figures 4 and 5 are $Z_{max} = 0.5$ cm, $Z_0 = 4.0$ cm, and $R_0 = 14.75$ cm.

Using the curve fits of the profiles for the density from (4) in (2), we obtain

$$\frac{2\epsilon_0 m}{e^2}\omega_0\Delta\omega = n_0\left\{\frac{\int_z[1-(\frac{z-Z_{max}}{Z_0})^2]\,dz}{l_0}\right\}\left\{\frac{\int_r[1-(\frac{r}{R_0})^4]|\mathbf{E}(r)|^2 r\,dr}{\int_r|\mathbf{E}(r)|^2 r\,dr}\right\}, \qquad (5)$$

where the field profiles are shown in figure 3. Using the best fit constants (given above) for the radial density data shown in figure 5, we obtain, for the braced term with the integrals over r, 1.20 for the 1.9 GHz resonance and 1.26 for the 2.6 GHz resonance. If we use the alternative analytic forms for the radial density variation (given in figure 5), the r integral factor becomes 1.55 for both resonances using the $1-(r/R_0)^2$ variation, and 1.77 for the 1.9 GHz resonance and 1.71 for the 2.6 GHz resonance using the J_0 variation. The small variation in these numbers indicates that the relative Langmuir probe measurements are not essential to obtain average plasma density, but are only needed if an accurate density profile is required. For the high frequency resonances where the plate spacing, l_0, is on the order of the free space wavelength, there may be a z dependence of $|\mathbf{E}|$, which would modify the z integrals in (5). As a worst case, if there is a symmetric half wavelength variation of $|\mathbf{E}|$ our data for n_0 must be multiplied by 0.680. Peak density (n_0) data for plasmas at 3 and 5 mT for powers in the range 10–100 W are shown in figure 6 and compared with simultaneous measurements using Langmuir probes.[13]

The two loop method of detecting the resonance shifts has the disadvantage that the loops must be inserted into the plasma cavity near the wall. We can, however, perform the measurements in another way to avoid this problem. We connect the network analyzer output to the grounded plate of the chamber through a high pass filter and observe the reflected signal. This is similar to the setup of de Vries, van Roosmalen, and Puylaert.[7] Results obtained with this method are very similar to those obtained with the loop excitation. Data

for a 10 mT plasma for powers in the range of 1–10 W are shown in figure 7. The power levels and thus the density were lower for this measurement, so lower frequency cavity resonances were used. The disagreement between the microwave results and the Langmuir probe results for this data is smaller than that obtained at the higher densities and is well within a factor of two.

IV . DISCUSSION AND CONCLUSIONS

We have shown that a cavity perturbation measurement can be performed in complex discharge geometries provided the frequency of the probing fields are well above the plasma frequency. By experimentally determining the density and field profiles, we can determine the peak density. The peak densities obtained with this method are about a factor of two smaller than the peak densities measured by a Langmuir probe. Considering the difficulty in measuring absolute density with a Langmuir probe, particularly in the presence of rf fields, it is not obvious which method gives the more accurate results. The two independent resonance measurements give data that agree with each other quite well, as seen in figure 6.

For accurate average density measurements it is necessary to measure the mode structure of the probing electric field, which can be combined with a reasonable density profile in the perturbation formula. Determination of the peak density requires more accurate plasma profile measurements, but would generally be less important a characteristic than the average density. Within a factor of two, the average density measurements are insensitive to both field and density profiles.

ACKNOWLEDGEMENTS

The authors wish to thank Arthur Sato and Blake Wood for performing the Langmuir probe measurements presented here. This work was supported by DOE Grant DE-FG03-87ER13727, National Science Foundation Grant ECS-8717363, and a National Science Foundation graduate fellowship.

REFERENCES

[1] B. Chapman, *Glow Discharge Processes,* (Wiley, New York, 1980)

[2] M. A. Biondi and S. C. Brown, Phys. Rev., **75**, (11), 1700–1705, 1949

[3] B. Agdur and B. Enander, J. Appl. Phys., **33**, (2), 575–581, 1962

[4] A. J. Lichtenberg, P. Govindan and J. R. Woodyard, J. Appl. Phys., **38**, (1), 382–389, 1967

[5] T. J. Bisschops, H. Störi, J. A. Engels, F. J. de Hoog and D. C. Schram, ISPC-7, Eindhoven, July 1985, paper number P-8-1

[6] M. A. Biondi, Phys. Rev., **109**, (6), 2005–2007, 1958

[7] C. A. M. de Vries, A. J. Roosmalen and G. C. C. Puylaert, J. Appl. Phys., **57**, (9), 4386–4390, 1985

[8] M. A. Lieberman and A. J. Lichtenberg, Phys. Fluids, **12**, (10), 2109–2116, 1969

[9] C. B. Fleddermann, J. H. Beberman and J. T. Verdeyen, J. Appl. Phys., **58**, (3), 1344–1348, 1985

[10] K. B. Persson, Phys. Rev., **106**, (2), 191–195, 1957

[11] G. Kent and D. Thomas, J. Appl. Phys., **41**, (12), 4945–4953, 1970

[12] J. C. Slater, Rev. Mod. Phys., **18**, 441, 1946

[13] R. R. J. Gagné and A. Cantin, J. Appl. Phys., **43**, (6), 2639–2647, 1972

FIGURES

Figure 1: Scale drawing of the cylindrical plasma discharge chamber. The electrode diameter is 22.9 cm, the inner diameter of the cavity is 30.2 cm, and the spacing l_0 between electrodes is 10 cm.

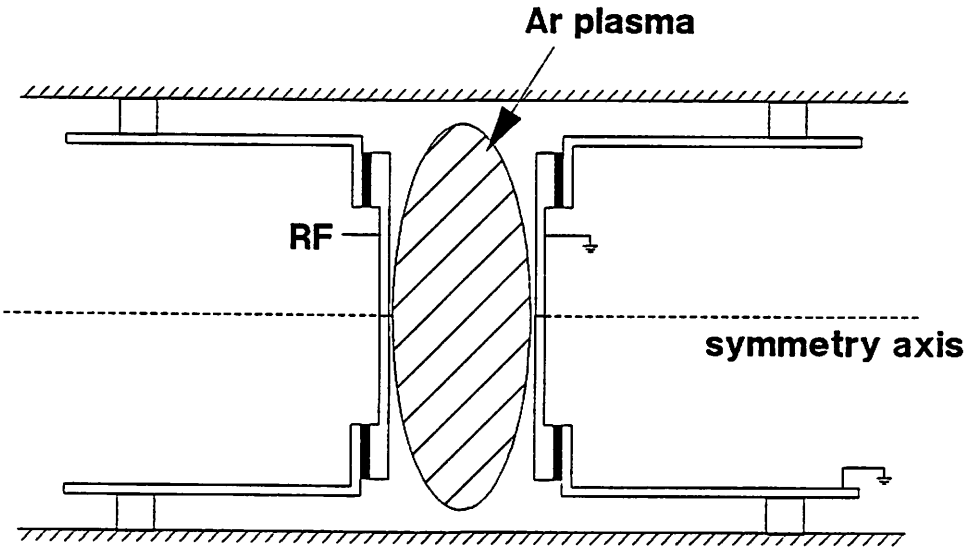

Figure 2: Microwave excitation system. The loops are inserted about 3.8 cm from the chamber wall. Dashed lines show the diameter connecting the probes and the two diameters used to measure the electric field magnitude.

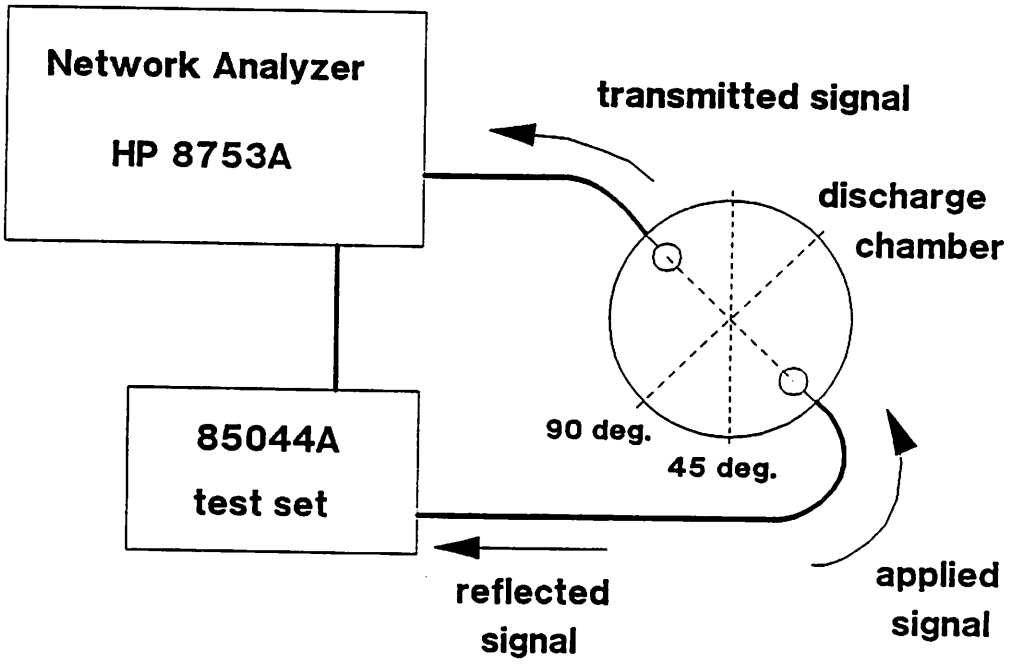

Figure 3a: Normalized |E| of 1.9 GHz resonance. Open circles represent the data taken along the diameter 90° from the probes. Data are subsequently fit to $\left|J_1(k_{11}r)\right|$, where $k_{11} = 0.253$ is the first zero of the J_1 Bessel function divided by the chamber radius R.

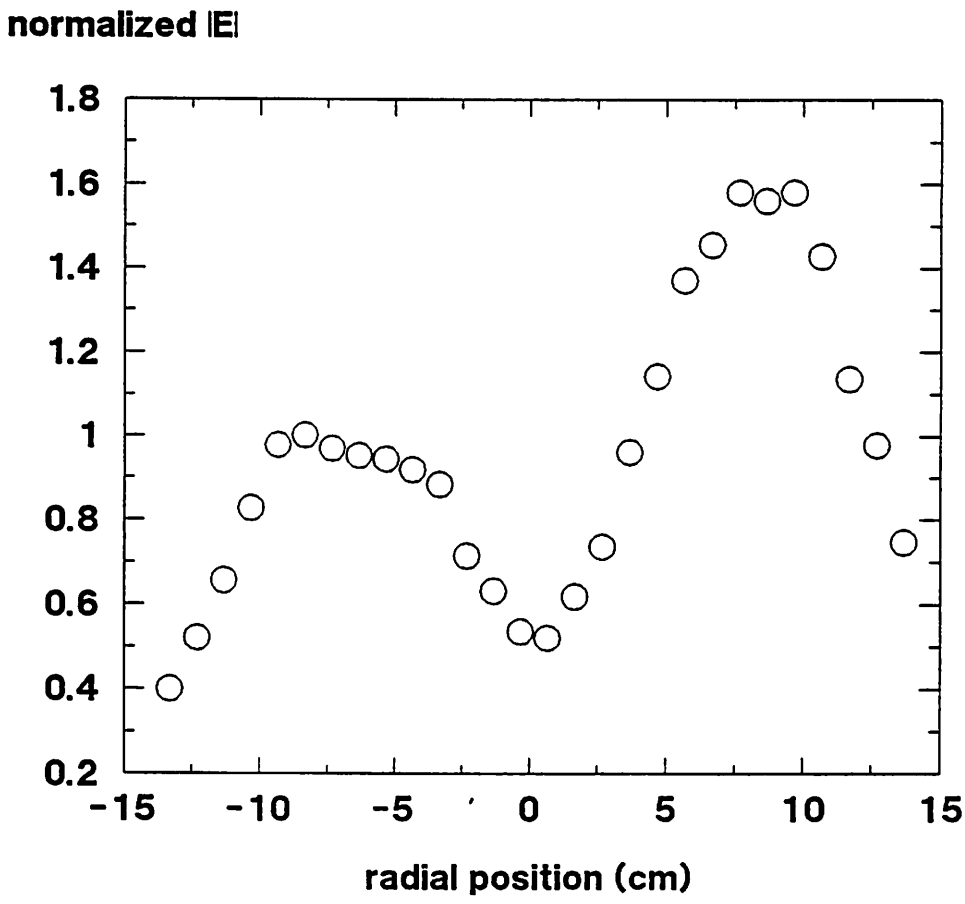

Figure 3b: Normalized |E| of 2.6 GHz resonance. Open circles represent the data taken along the diameter 90° from the probes. Data are subsequently fit to $\left|J_1(k_{12}r)\right|$, where $k_{12} = 0.463$ is the second zero of the J_1 Bessel function divided by the chamber radius R.

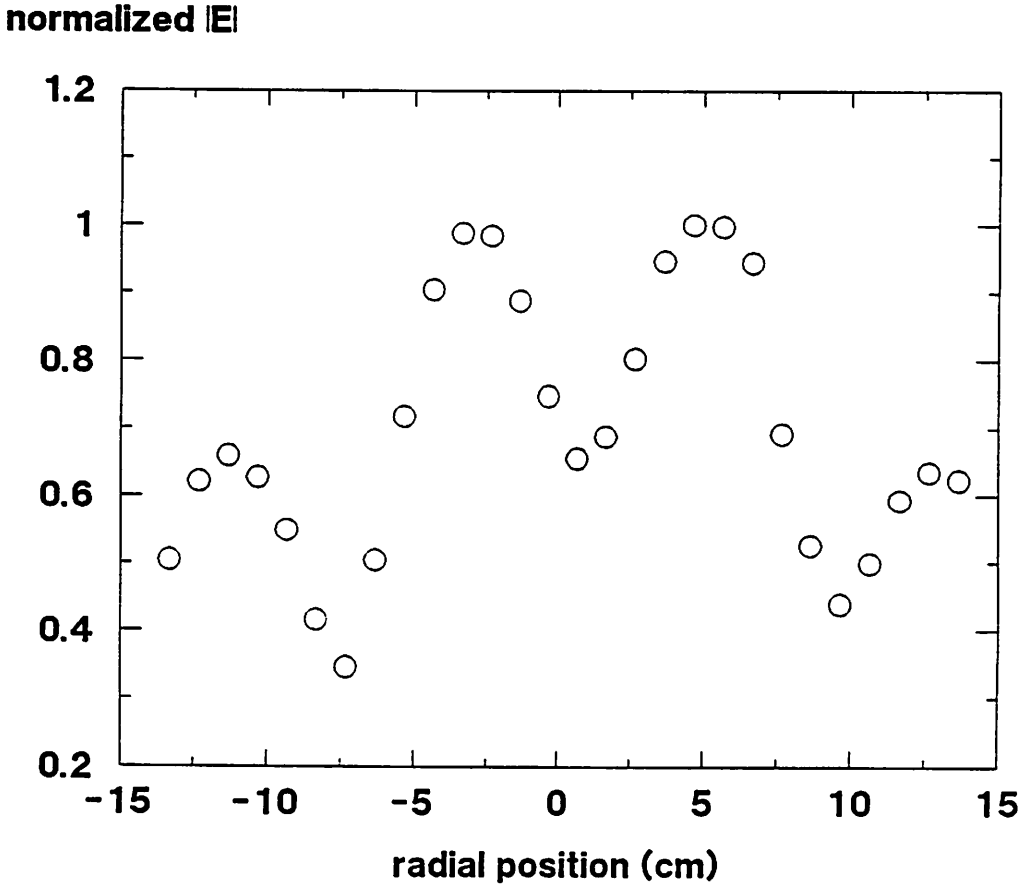

Figure 3c: Normalized |**E**| of 443 MHz resonance. Open circles represent the data taken along the diameter 90° from the probes, and open squares the data taken along the diameter 45° from the probes. Both sets of data are subsequently fit to $1-(\frac{r}{R})^2$, where R is the chamber radius.

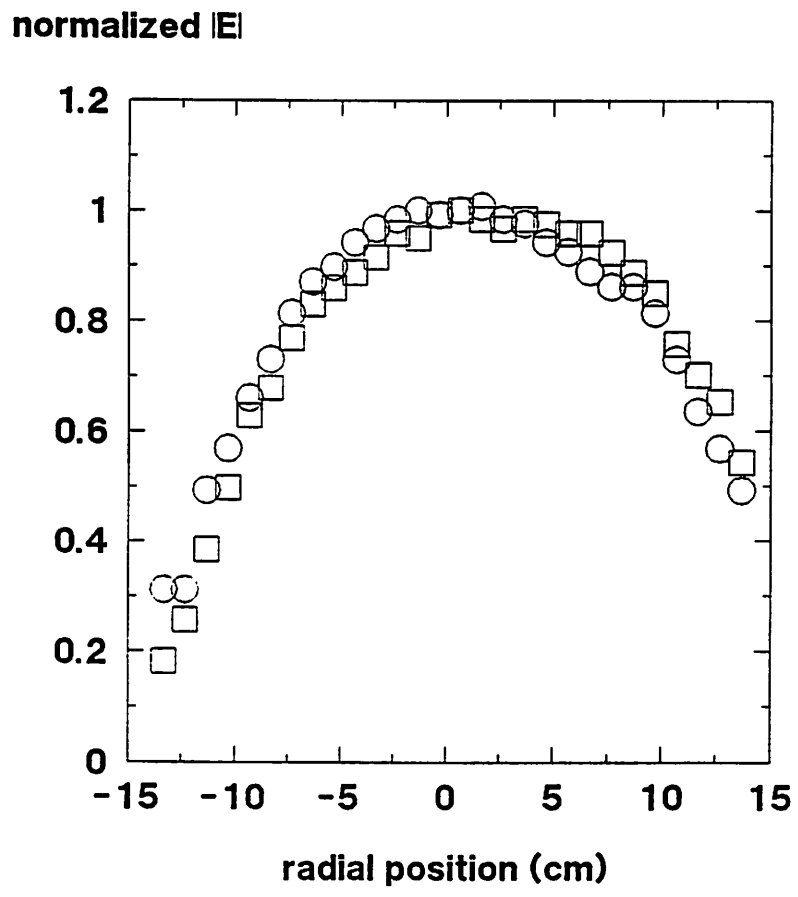

Figure 3d: Normalized |E| of 506 MHz resonance. Open circles represent the data taken along the diameter 90° from the probes, and open squares the data taken along the diameter 45° from the probes. Both sets of data are subsequently fit to $1 - (\frac{|r|-R}{R})^2$, where R is the chamber radius.

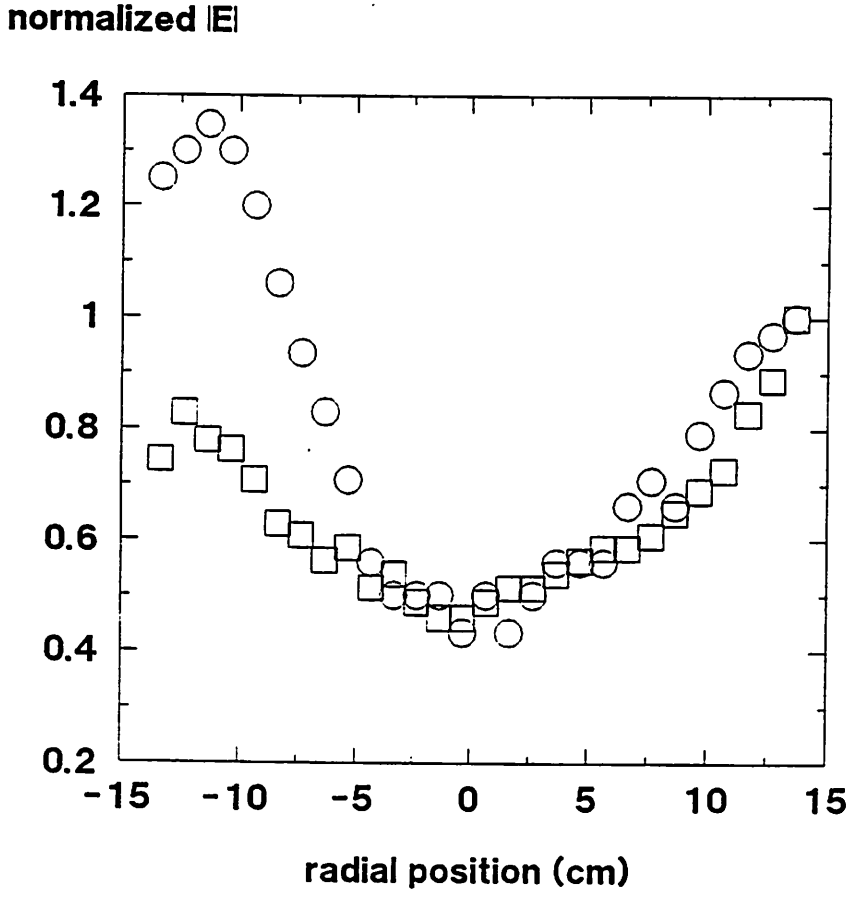

Figure 4: Normalized z variation of density. Open circles and open squares represent two different sets of Langmuir probe density data. The powered electrode is at -5 cm, and the grounded electrode at 5 cm. Sheaths are at approximately -3.5 and 4.5 cm. A quadratic fit to the data is shown by the solid line.

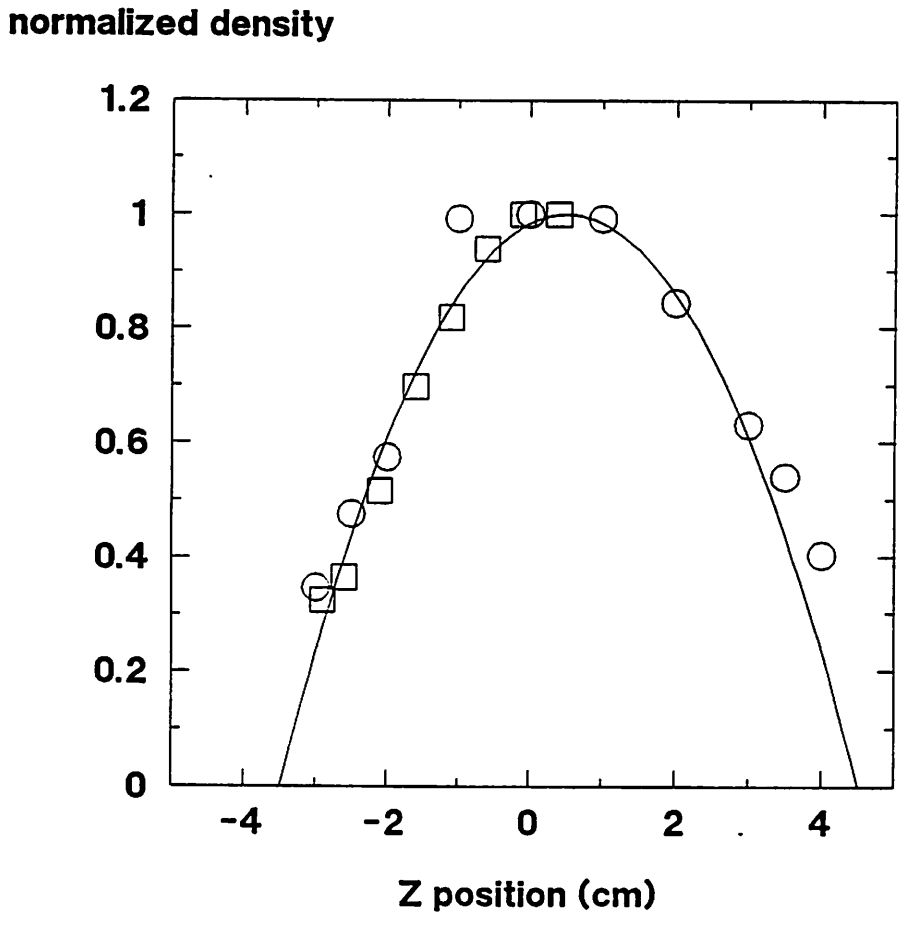

Figure 5: Normalized r variation of density. Open circles represent the Langmuir probe density data. The sheath is observed to be at about $R_0 = 14.75$ cm. Three different curve fits are shown for the data: the solid line is a plot of $1-(r/R_0)^4$, the dashed line a plot of $1-(r/R_0)^2$, and the dotted–dashed line a plot of $J_0(k_{01}r)$, where $k_{01} = 0.163$ is the first zero of the J_0 Bessel function divided by R_0. All fits have a zero slope at $r = 0$ and go to zero at the sheath edge.

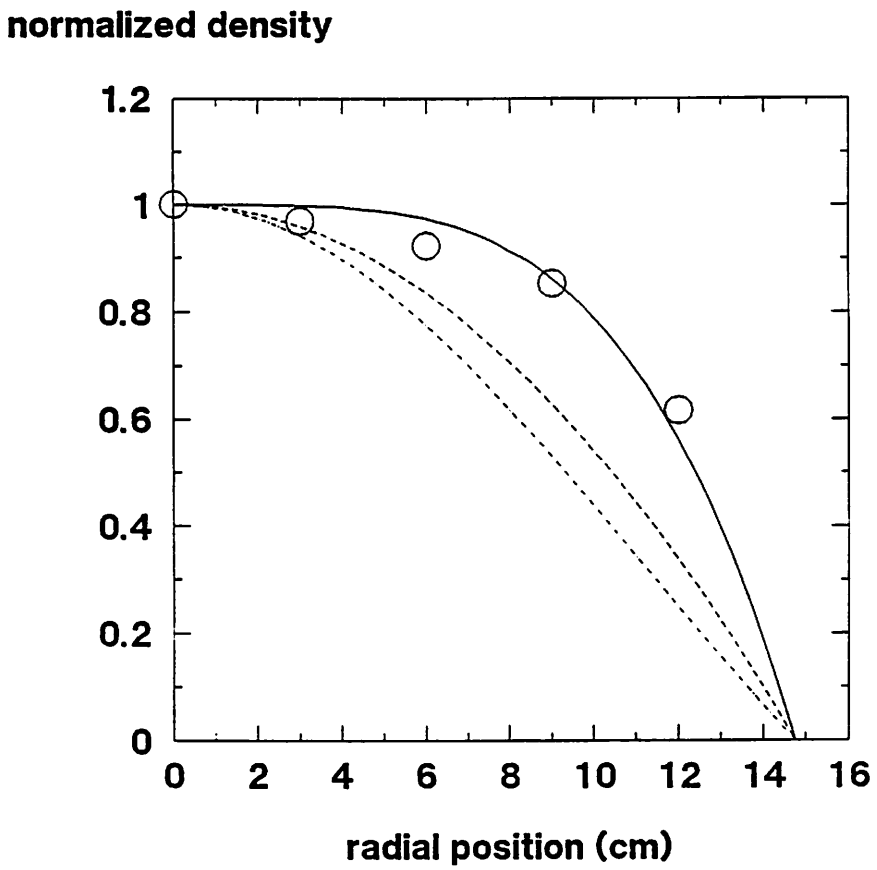

Figure 6a: Density versus power, two loop method. Open circles represent data from the 1.9 GHz resonance, open squares data from the 2.6 GHz resonance, and open triangles data from the Langmuir probe. Data are for a 3 mT plasma.

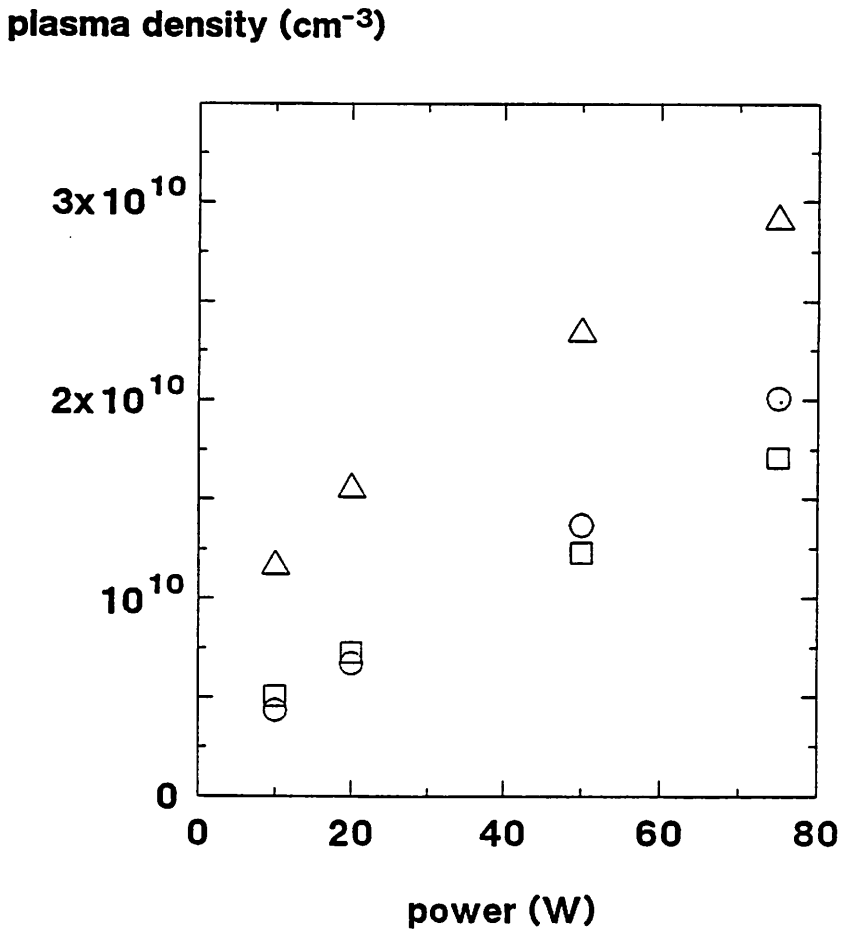

Figure 6b: Density versus power, two loop method. Open circles represent data from the 1.9 GHz resonance, open squares data from the 2.6 GHz resonance, and open triangles data from the Langmuir probe. Data are for a 5 mT plasma.

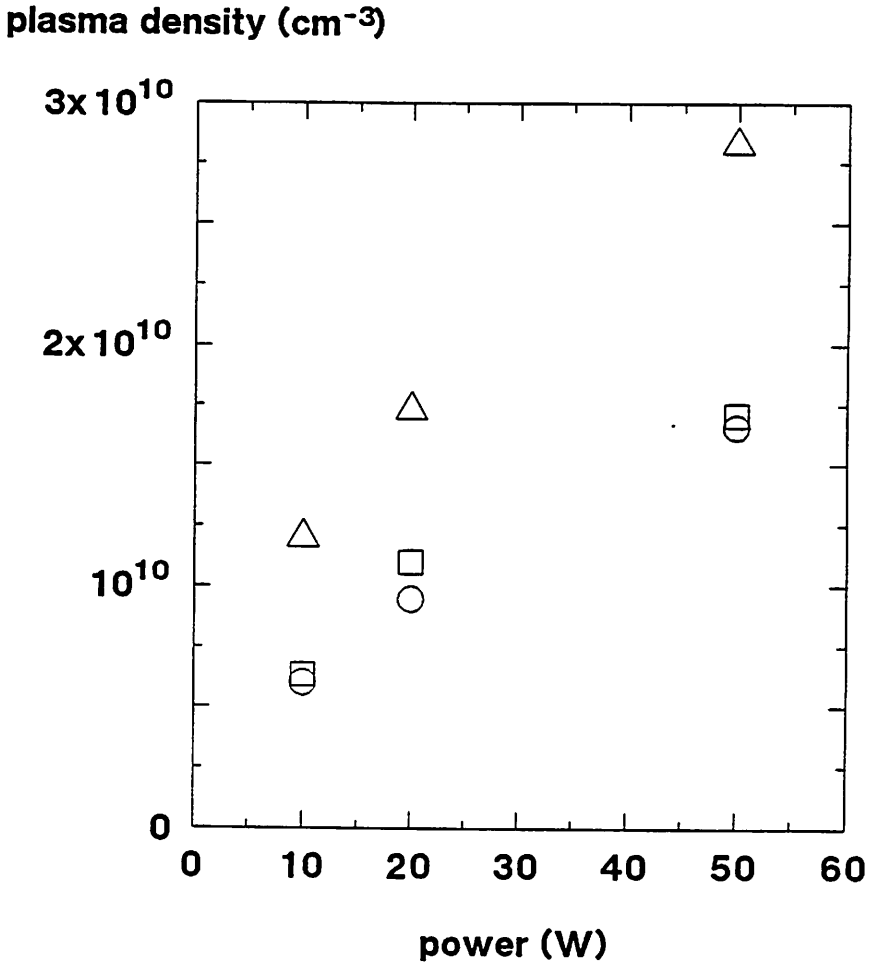

Figure 7: Density versus power, ground electrode reflection method. Open circles represent data from the 443 MHz resonance, open squares data from the 506 MHz resonance, and open triangles data from the Langmuir probe. Data are for a 10 mT plasma.